Chapter 6
Evaluation of Photocatalytic Activity of the TiO_2 Layer Formed on Ti by Thermal Oxidation

Takayuki Narushima, Shota Sado, Natsumi Kondo, Kyosuke Ueda, Mitsuko Kawano, and Kouetsu Ogasawara

Abstract Two-step thermal oxidation was proposed for Ti and Ti alloys as a surface-treatment process for preparing an anatase-containing TiO_2 layer. This process consisted of treatment in a CO-containing atmosphere (first step) and subsequent treatment in air (second step). In this chapter, first, the current status of TiO_2 coating onto Ti and Ti alloys for biomedical applications is reviewed; then our recent work on the phase and microstructure of TiO_2 layers prepared on commercially pure (CP) Ti, Ti-25mass%Mo alloy, and Ti-25mass%Nb alloy by two-step thermal oxidation is described. The anatase fraction in the TiO_2 layer was controlled through process parameters such as the second-step temperature. Finally, photocatalytic activity of TiO_2 layers formed on the Ti and Ti alloys is evaluated, including: results of water contact angle, decomposition of methylene blue, and antibacterial effects.

Keywords Anatase • Antibacterial activity • Photocatalytic activity • Thermal oxidation • Ti and Ti alloys

T. Narushima (✉) • S. Sado • N. Kondo • K. Ueda
Department of Materials Processing, Tohoku University, Sendai 980-8579, Japan
e-mail: narut@material.tohoku.ac.jp

M. Kawano
Department of Immunobiology, Institute of Development, Aging and Cancer, Tohoku University, Sendai 980-8575, Japan

K. Ogasawara
Department of Immunobiology, Institute of Development, Aging and Cancer, Tohoku University, Sendai 980-8575, Japan

Department of Intractable Diseases and Immunology, Tohoku University, Sendai 980-8575, Japan

K. Sasaki et al. (eds.), *Interface Oral Health Science 2014*,
DOI 10.1007/978-4-431-55192-8_6

6.1 Introduction

Ti and Ti alloys are important metallic biomaterials as well as stainless steels and Co-Cr alloys because of their excellent properties such as high specific strength, high corrosion resistance, and low allergenicity [1, 2]. Since they can be directly connected to living bone at an optical microscopic level, i.e., osseointegration [3, 4], they have been used as substitutes for hard tissues such as in the stems of artificial hip joints and in dental implants, where implantation in bones for the long-term is expected. However, a relatively long time is required for establishing osseointegration, and fixation between Ti implants and bones can be influenced by the state of the bones and by the implant/bone interfacial area. Surface modification is a promising way to improve bone compatibility of Ti implants [5], while leaving bulk mechanical properties intact.

Surface modification used to improve bone compatibility of Ti implants is conducted from the point of view of the morphology and phase/composition of their surfaces [6–8]. The aim of modifying surface morphology is to increase adhesion between bones and implants by an anchorage effect, while the purpose of phase/composition modification is to form either an apatite coating, or a non-apatite coating that enhances the formation of apatite [7].

We have reported amorphous calcium phosphate coating using RF magnetron sputtering [8–10], and TiO_2 coating using thermal oxidation [11–13], as surface modifications of Ti and Ti alloys for biomedical applications. In this chapter, first, the current status of TiO_2 coating of Ti and Ti alloys is reviewed, and then our recent work on preparation and evaluation of photocatalytic activity of TiO_2 layers on Ti and Ti alloys formed by a two-step thermal oxidation process is described.

6.2 TiO_2 Layers on Ti and Ti Alloys for Biomedical Applications

TiO_2 layers on Ti and Ti alloys are reported to be effective for improving biological performance such as biomimetic growth of apatite [14], initial adhesion of osteoblast-like cells [15], bone-bonding ability [16], and bone growth [17]; in fact, Ti implants coated with a porous TiO_2 layer through anodic oxidation are clinically used [18]. It is known that TiO_2 can exhibit photocatalytic activity [19, 20]. Photo-induced superhydrophilicity and photocatalytic oxidation of organic compounds are closely related to biological phenomena on the TiO_2 surface such as cell response, removal of hydrocarbons, and antibacterial properties [21–23].

TiO_2 has three polymorphic phases at atmospheric pressure: rutile, anatase, and brookite. Rutile is a thermodynamically stable phase on the macroscale, with the stability of these phases depending on particle size. Rutile and anatase are the most stable phase for particles above 35 nm and below 11 nm, respectively, and

brookite has been found to be the most stable for nanoparticles in the 11–35 nm range [20, 24]. Anatase is considered to possess excellent bone compatibility [14, 16, 25], and the photocatalytic activities of anatase [19, 26], anatase + rutile composite [27], and anatase + brookite composite [28] are reported to be high, although the precise reason for different photocatalytic activities has not been elucidated in detail [20].

Many processes for preparing TiO_2 layers on Ti and Ti alloys have been investigated including chemical vapor deposition [29], physical vapor deposition [30], anodic oxidation/micro arc oxidation (MAO) [31, 32], and sol–gel [33] methods. Thermal oxidation, which is based on the reaction between an oxidizing gas and Ti at elevated temperatures, is a simple and low-cost method to prepare TiO_2 layers on Ti with excellent adherence and high crystallinity, and can be applied to substrates with a complex geometry.

The thermal oxidation of commercially pure (CP) Ti in air and oxygen has been reported since the 1950s [34]. Recently, the oxide layer on Ti and/or the oxygen-dissolved and hardened layer of Ti prepared by thermal oxidation have been utilized for improving corrosion and wear resistance [35–37]. Browne and Gregson [38] showed that the air oxidation treatment at 673 K for 2.7 ks for Ti-6Al-4V implants reduced metal ion dissolution into bovine serum, particularly in the early stages.

The major product obtained in the thermal oxidation of Ti and Ti alloys has been reported to be the thermodynamically stable rutile [37]. A few reports show formation of the anatase phase in thermal oxidation of Ti and Ti alloys [39, 40]. Borgioli et al. [39] reported the formation of rutile + anatase in the oxide film on a Ti–6Al–4V alloy after glow-discharge processing in air at a total gas pressure of 0.01 atm. Lee and Park [40], using oxidation in a wet oxygen atmosphere for 10.8 ks at 683 K in combination with post-annealing in air at 773 K, showed formation of a Ti_5O_7 + anatase layer on a magnetron-sputtered Ti thin film. In these reports, however, the main oxidation products were rutile and Ti_5O_7 phases, namely, not an anatase-rich TiO_2 layer.

On the other hand, it is known that anatase is formed as a main product in thermal oxidation of TiC [41, 42] and TiN [43]. Shabalin et al. [42] presented an oxidation model of TiC, in which incorporation of carbon in TiO_2 stabilized the anatase phase. Meanwhile, Kao et al. [44] observed the reversible transformation between TiO having an NaCl-type structure and anatase. They pointed out the similarity between their structures: TiC and TiN exhibit NaCl type structure with a lattice constant close to TiO; the anatase formation on TiC and TiN in thermal oxidation would be related to this NaCl-type structure.

Based on the information on anatase formation on TiC and TiN under thermal oxidation, we proposed and investigated a two-step thermal oxidation process in which an anatase-rich TiO_2 layer is formed on Ti and Ti alloys [11–13]. The preparation and photocatalytic evaluation of TiO_2 layers formed on Ti and Ti alloys by two-step thermal oxidation are described in Sects. 6.3 and 6.4, respectively.

6.3 Preparation of Anatase-Rich TiO_2 Layer on Ti and Ti Alloys

Figure 6.1 schematically shows the process of two-step thermal oxidation. This process consists of treatment in CO-containing atmospheres such as Ar-CO [11] and N_2-CO [12] gas mixtures (first step) and subsequent treatment in air (second step). A Ti(C,O) or Ti(C,N,O) phase is formed on the Ti and Ti alloys in the first step and converted to TiO_2 through air oxidation in the second step.

The α-2θ XRD patterns ($\alpha = 0.3°$, Cu Kα) of the reaction layer on CP Ti, Ti-25mass%Mo (Ti-25Mo) alloy, and Ti-25mass%Nb (Ti-25Nb) alloy after the first-step treatment in Ar-1%CO at 1,073 K for 3.6 ks are shown in Fig. 6.2. Reflections that are located close to but at a slightly higher angle than those of TiC are observed. It is known that oxygen substitution in a carbon site decreases the lattice parameter of TiC [42]; in fact, the reflections of the reaction layer are located between those of TiC and TiO as shown in Fig. 6.2. In addition, chemical composition analysis by X-ray photoelectron spectroscopy (XPS) revealed the presence of oxygen in the reaction layer as well as carbon and Ti [11]. From these results, the phase of the reaction layer is considered to be Ti(C,O). In the case of using an N_2-CO gas atmosphere in the first step, a Ti(C,N,O) reaction layer was formed [12]. Figure 6.3a, b depict potential diagrams of Ti-C-O and Ti-C-N-O systems respectively, at 1,100 K [11, 12]. The chemical composition of Ti(C,O) and Ti(C,N,O) phases was arbitrarily chosen as $TiC_{0.5}O_{0.5}$ because of the lack of reliable thermodynamic data for these phases. The relationship between carbon activity (a_C) and oxygen partial pressure (P_{O_2}) suggests that the $TiC_{0.5}O_{0.5}$ phase is thermodynamically stable at a CO partial pressure (P_{CO}) of 0.01 atm, which corresponds to Ar-1%CO and N_2-1%CO.

Figure 6.4 shows cross-sectional SEM images of the Ti(C,O) and Ti(C,N,O) layers, which were formed in Ar-1%CO and N_2-1%CO, respectively. From the images, it was confirmed that the films were dense and uniform.

The phase fraction in TiO_2 layers formed on CP Ti, Ti-25Mo alloy, and Ti-25Nb alloy at different second-step temperatures and holding times are summarized in

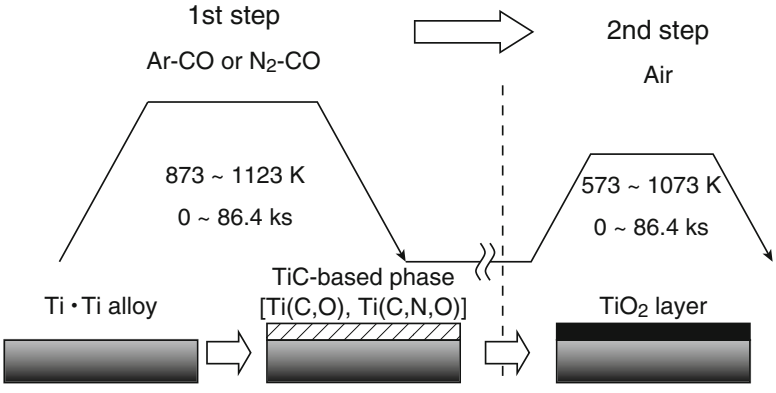

Fig. 6.1 Schematic of the two-step thermal oxidation process

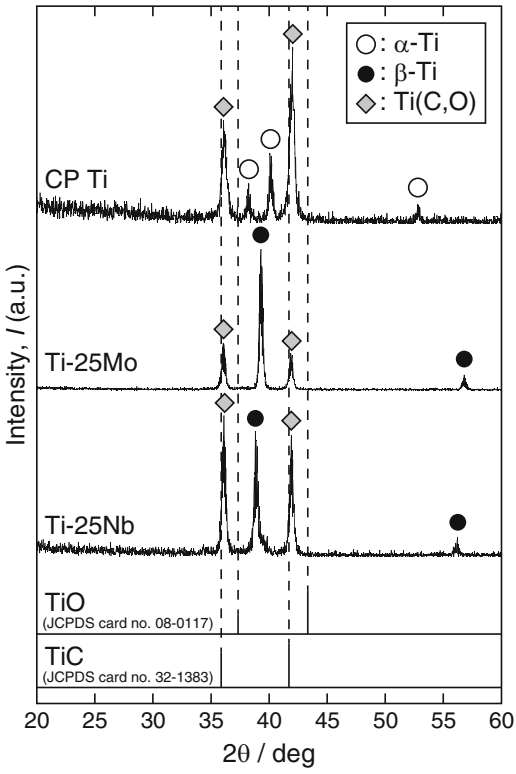

Fig. 6.2 α-2θ XRD patterns of the reaction layers on CP Ti, Ti-25Mo alloy, and Ti-25Nb alloy after first-step treatment in Ar-1%CO at 1,073 K for 3.6 ks

Fig. 6.5a–c, respectively [13]. The first-step treatment was carried out in Ar-1%CO at 1,073 K for 3.6 ks, and the reaction layer was confirmed to be Ti(C,O) single phase after the first-step. The phase fractions of anatase and rutile in TiO_2 layer were calculated using the equation given by Spurr and Myers [45]. The anatase-rich TiO_2 layers were formed for second-step temperatures between 673 and 873 K. At a lower temperature of 573 K, single-phase anatase was produced, but the Ti(C,O) phase remained, indicating that the oxidation reaction from Ti(C,O) to TiO_2 was not completed in the second step. On the other hand, thermodynamically stable rutile was a main phase in the TiO_2 layers for the higher second-step temperatures of 973 and 1,073 K. At these higher temperatures, rutile single phase was detected on CP Ti, while anatase was detected as a minor phase on Ti-25Mo and Ti-25Nb alloys. Moreover, the anatase fraction in the TiO_2 layer on Ti-25Mo and Ti-25Nb alloys was higher than on CP Ti at mid-level temperatures of 773 and 873 K. The formation window for anatase in two-step thermal oxidation of Ti alloys is wider than that of CP Ti.

Anatase irreversibly transforms to rutile at high temperatures, and the larger the valence number and ionic radius of dopants in TiO_2, the more suppressed the anatase-to-rutile transformation: the transformation is enhanced by relaxation of the large oxygen sublattice through the increased presence of oxygen vacancies [46].

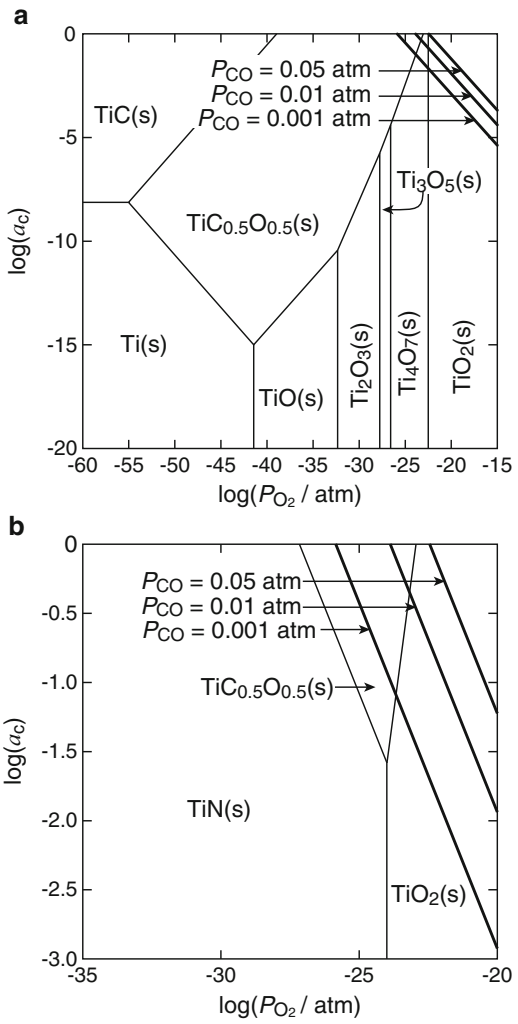

Fig. 6.3 Potential diagrams for the (**a**) Ti-C-O system and (**b**) Ti-C-N-O system (N_2 pressure: 0.1 MPa) at 1,100 K [11, 12]

Figure 6.6 shows the comprehensive valence/radius plot of the anatase-to-rutile transformation, categorizing TiO_2 dopants as inhibiting or promoting [46]. From this figure, Mo and Nb are likely inhibiting dopants. The incorporation of Mo and Nb into the TiO_2 layer during two-step thermal oxidation process may have resulted in the presence of anatase on the Ti alloys at higher second-step temperatures and the higher anatase fraction at mid-level temperatures.

The formation of the Ti(C,O) or Ti(C,N,O) single phase during the first step and optimization of the second-step temperature are required for preparing an anatase-rich TiO_2 layer on Ti and Ti alloys. We varied CO partial pressures in the first-step treatment between Ar- or N_2-0.1%CO and 20%CO. The rutile phase tended to form to a greater degree in the first-step treatment under higher partial pressures (up to 20 %) of CO gas, because of its high oxidizing potential.

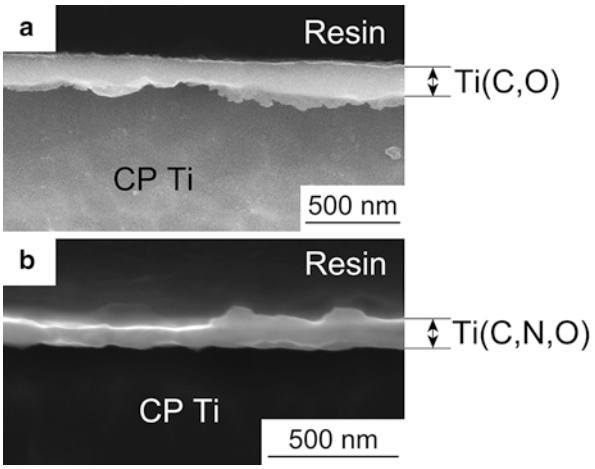

Fig. 6.4 Cross sections of (**a**) Ti(C,O) and (**b**) Ti(C,N,O) layers on CP Ti after the treatments in Ar-1%CO and N_2-1%CO, respectively [11, 12]

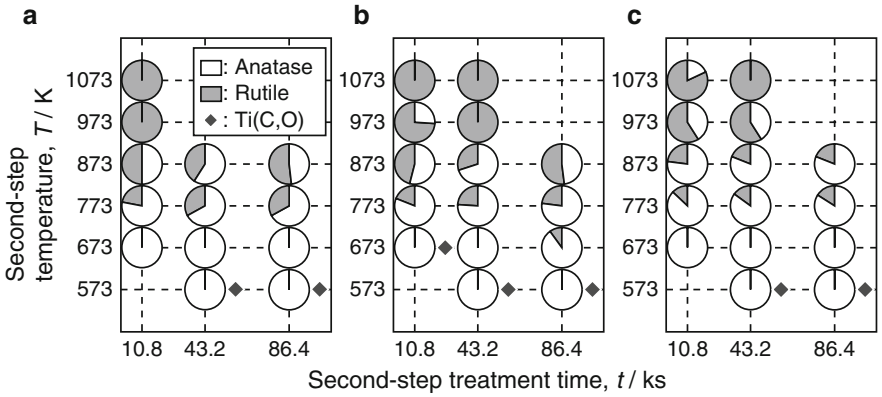

Fig. 6.5 Phase fraction of the reaction layer on (**a**) CP Ti, (**b**) Ti-25Mo alloy, and (**c**) Ti-25Nb alloy after the second-step treatment in air [13]. *Grey* and *white* parts in *small circles* show rutile and anatase fractions, respectively

Figure 6.7a, b show a cross-sectional TEM image and an electron diffraction pattern, respectively, of the anatase + rutile TiO_2 layer formed on CP Ti after a second-step treatment at 673 K that was preceded by a first-step treatment at 1,073 K in N_2-1%CO [12]. Nanoscale crystallites of anatase and rutile are observed. The thickness of the TiO_2 layer formed in the second-step at 873 K was much greater than that formed in the 573–773 K range [12]. This result suggests that the formation of the rutile phase at higher second-step temperatures is also caused by direct oxidation of metallic Ti after completion of oxidation of the Ti(C,O) or Ti(C,N,O) layer.

Bonding strength of the anatase-rich TiO_2 layer to the CP Ti substrate was evaluated by a pulling test using an Al stud, and was greater than the strength of the epoxy glue (60–70 MPa) used for bonding between the TiO_2 layer and the Al stud [14]. The high bonding strength is an advantage of the thermal oxidation process over wet processes such as anodic oxidation.

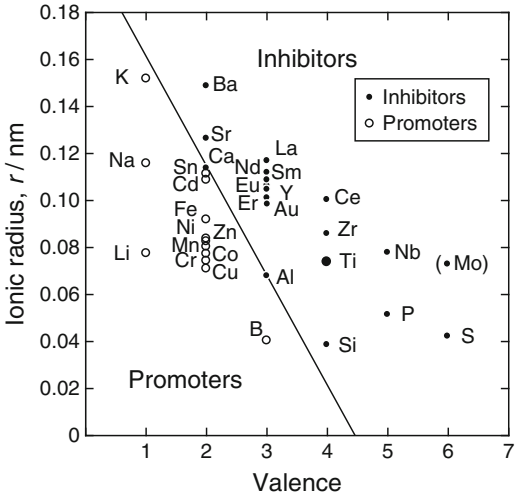

Fig. 6.6 Comprehensive valence/radius plot of anatase-to-rutile transformation, categorizing dopants as inhibiting or promoting [46]

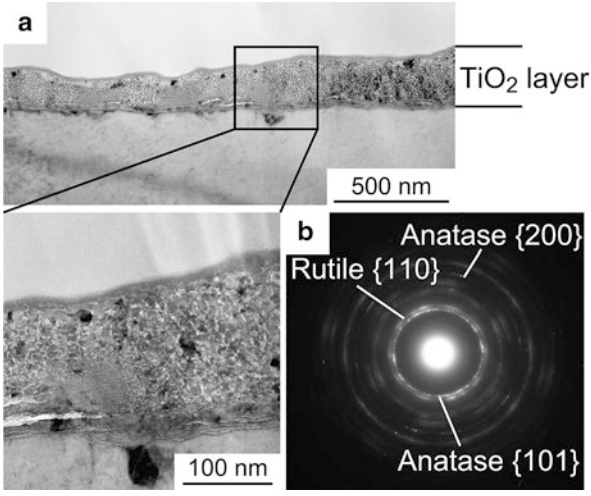

Fig. 6.7 (**a**) Cross-sectional TEM image and (**b**) electron diffraction pattern of the TiO_2 layer formed on CP Ti after two-step thermal oxidation [12]

6.4 Evaluation of Photocatalytic Activity of TiO_2 Layers Formed by Two-Step Thermal Oxidation

The photocatalytic activity of TiO_2 layers prepared on CP Ti, Ti-25Mo alloy, and Ti-25Nb alloy was evaluated for water contact angle, decomposition of methylene blue (MB), and antibacterial effect under UV irradiation. Figure 6.8 shows the average water contact angle obtained for UV irradiation times of 3.6–7.2 ks with an irradiance of 1 $mW \cdot cm^{-2}$ as a function of anatase fraction (f_A) in TiO_2 layers [13]. The water contact angle decreased with increasing f_A, and in particular, a water contact angle less than 5° was achieved on TiO_2 layers for an f_A higher than 0.6.

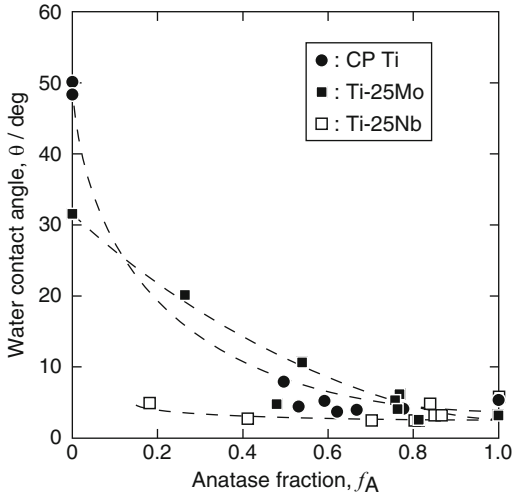

Fig. 6.8 Variation in water contact angle with anatase fraction (f_A) of the TiO_2 layer under UV irradiation [13]

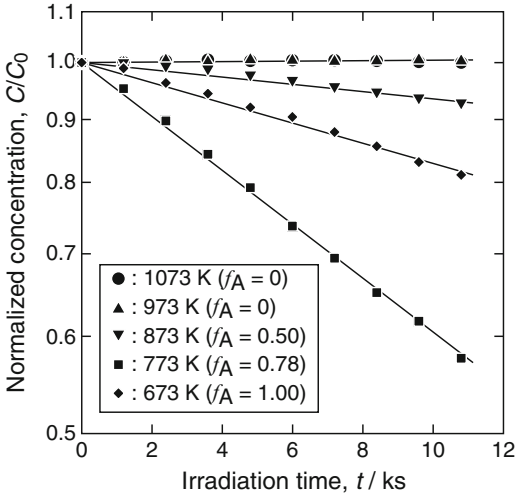

Fig. 6.9 Degradation of methylene blue under UV irradiation on the TiO_2 layer with different anatase fractions (f_A) formed on CP Ti

It is confirmed that anatase is effective for expression of superhydrophilicity. Meanwhile, in the case of Ti-25Nb alloy, a low water contact angle was observed even on TiO_2 layers with lower f_A values such as 0.2 and 0.4. The effect of Nb doping on the photocatalytic activity of TiO_2 was reported to be complex [47]. Further studies on the chemical state, concentration, and distribution of Nb in the TiO_2 layer are required. The water contact angle increased again under dark condition after UV irradiation; however, the hydrophobization rate was reduced in TiO_2 layers with high f_A.

Figure 6.9 shows the variation in concentration of MB with UV irradiation time on TiO_2 layers formed on CP Ti, Ti-25Mo alloy, and Ti-25Nb alloy. The values of

f_A in the TiO_2 layers were controlled by varying the second-step temperature between 673 and 1,073 K. The rate constants for degradation of MB can be expressed by the gradients of the lines in Fig. 6.9. The anatase-containing TiO_2 layers exhibited higher decomposition rates compared to the rutile single-phase TiO_2 layers. The maximum rate constant was obtained at the f_A value of 0.78. Bickley et al. [48] proposed a synergetic effect between anatase and rutile in order to explain a greater photocatalytic activity of anatase + rutile + amorphous TiO_2 particles. Su et al. [49] reported that porous TiO_2 films with an f_A value of 0.6 exhibited optimal performance of photocatalytic activity and suggested a synergetic effect on photocatalytic activity: electrons excited in rutile can migrate to the conduction band of anatase, thereby effectively suppressing recombination of electrons and holes [49].

Antibacterial activities of a CP Ti plate coated with anatase single-phase TiO_2 layer by two-step thermal oxidation (Anatase-coated, $10 \times 10 \times 1$ mm) and an as-polished CP Ti plate (Non-coated, $10 \times 10 \times 1$ mm) were evaluated using gram-positive *E. coli* (DH 5α). All specimens were ultrasonically cleaned and sterilized in ethanol for 0.6 ks before the antibacterial tests. Solution (0.1 mL) containing the bacteria at a concentration of 10^7 CFU $\cdot$ mL^{-1} diluted using 1/500 nutrient broth (NB) was dropped onto the specimen in a 24-well plate. The specimen was exposed to UV with an irradiance of 0.25 mW $\cdot$ cm^{-2} at 298 ± 5 K in a dark room. After 10.8 ks incubation, the dropped bacterial solution was washed out from the specimen using 4.9 mL of phosphate buffered saline (PBS). The washed-out solution (0.1 mL) including bacteria was inoculated onto a standard NB agar culture plate ($\phi = 90$ mm). The number of colonies resulting from the growth of viable bacteria was counted after incubation for 64.8 ks at 310 K, and the number of viable bacteria (N_{sp}) was calculated. The same protocol was conducted with the well plate without specimen and the number of viable bacteria (N_{well}) was also calculated. A percentage of viable bacteria (P_v) was evaluated using a following equation.

$$P_v = N_{sp}/N_{well} \times 100 \tag{6.1}$$

Significant differences were statistically evaluated using Student's *t*-test.

Figure 6.10 shows the percentage of viable bacteria for the Non-coated and Anatase-coated specimens. The percentage of viable bacteria for Anatase-coated was significantly lower than for Non-coated. This result indicates that the anatase layer on Ti formed by two-step thermal oxidation is useful to improve the antibacterial activity of Ti implants. Many research groups have reported antibacterial activity of an anatase layer on Ti formed by anodic oxidation [50–52]. We have showed significant antibacterial activity of an anatase layer on Ti formed by a dry process: two-step thermal oxidation.

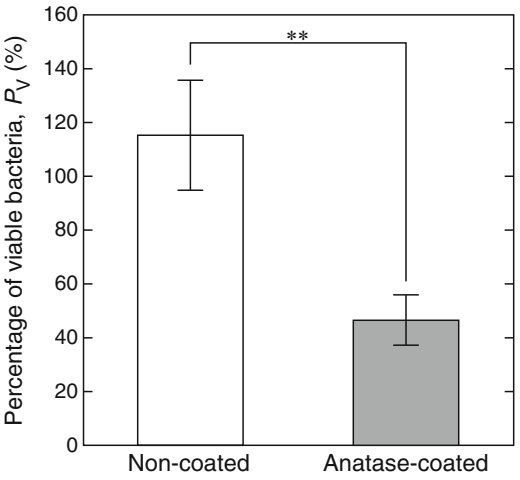

Fig. 6.10 Percentage of viable bacteria of CP Ti plate coated with anatase single-phase TiO_2 layer (Anatase-coated) and as-polished CP Ti plate (Non-coated). (**$p < 0.01$)

6.5 Summary

TiO_2 layers formed by thermal oxidation can improve the biological properties of Ti through their photocatalytic activity. Research and development of TiO_2 coatings on Ti implants for hard tissue replacement is continuing. In applications of TiO_2-coated Ti implants, it would be preferable if the photocatalytic response of TiO_2 layers were to visible light. Theoretical and experimental studies are needed to further improve photocatalytic activity and clarify the detailed mechanism of photocatalytic activity of TiO_2 layers on Ti, which would relate to phase fraction, defect structure, and dopants. In particular, precise microscopic analyses of the structure and composition of TiO_2 thin layers on Ti are needed to aid in understanding their photocatalytic properties.

Acknowledgements This study was partially supported by a Grant-in-Aid for Scientific Research from the Ministry of Education, Culture, Sports, Science and Technology (MEXT), Japan.

References

1. Niinomi M, Hanawa T, Narushima T. Japanese research and development on metallic biomedical, dental, and healthcare materials. JOM. 2005;57(4):18–24.
2. Niinomi M. Recent metallic materials for biomedical applications. Metall Mater Trans A. 2002;33:477–86.
3. Brånemark P-I, Hansson BO, Adell R, Breine U, Lindström J, Hallén O, Öhman A. Osseointegrated implants in the treatment of the edentulous jaw, experience from a 10-year period. Scand J Plast Reconstr Surg Suppl. 1977;16:1–132.

4. Brånemark P-I. Osseointegration and its experimental background. J Prosthet Dent. 1983;50:399–410.
5. Goto T, Narushima T, Ueda K. Bio-ceramic coating on titanium by physical and chemical vapor deposition. In: Zhang S, editor. CRC handbook of biological and biomedical coatings. Boca Raton: CRC; 2011. p. 299–332.
6. Narushima T, Ueda K. Calcium phosphate coating on titanium by RF magnetron sputtering. In: Wu J, editor. Technological advancements in biomedicine for healthcare applications. Hershey: IGI Global; 2012. p. 223–33.
7. Hanawa T. Research and development of metals for medical devices based on clinical needs. Sci Technol Adv Mater. 2012;13:064102.
8. Narushima T, Ueda K, Goto T, Masumoto H, Katsube T, Kawamura H, Ouchi C, Iguchi Y. Preparation of calcium phosphate films by radiofrequency magnetron sputtering. Mater Trans. 2005;46:2246–52.
9. Ueda K, Narushima T, Goto T, Taira M, Katsube T. Fabrication of calcium phosphate films for coating on titanium substrates heated up to 773K by RF magnetron sputtering and their evaluations. Biomed Mater. 2007;2:S160–6.
10. Shiraishi N, Rong T, Uzuka R, Narushima T, Goto T, Niinomi M, Sasaki K, Suzuki O. Biomechanical evaluation of amorphous calcium phosphate coated TNTZ implants prepared using a radiofrequency magnetron sputtering system. Mater Trans. 2012;53:1343–8.
11. Okazumi T, Ueda K, Tajima K, Umetsu N, Narushima T. Anatase formation on titanium by two-step thermal oxidation. J Mater Sci. 2011;46:2998–3005.
12. Umetsu N, Sado S, Ueda K, Tajima K, Narushima T. Formation of anatase on commercially pure Ti by two-step thermal oxidation using N_2-CO gas. Mater Trans. 2013;54:1302–7.
13. Narushima T, Ueda K, Sado S. Surface treatment of titanium using thermal oxidation for biomedical applications. Corr Eng Jpn. 2014;63:295–300.
14. Lin C-M, Yen S-K. Biomimetic growth of apatite on electrolytic TiO_2 coatings in simulated body fluid. Mater Sci Eng C. 2006;26:54–64.
15. Yang X-F, Chen Y, Yang F, He F-M, Zhao S-F. Enhanced initial adhesion of osteoblast-like cells on an anatase-structured titania surface formed by H_2O_2/HCl solution and heat treatment. Dent Mater. 2009;25:473–80.
16. Liang B, Fujibayashi S, Neo M, Tamura J, Kim H-M, Uchida M, Kokubo T, Nakamura T. Histological and mechanical investigation of the bone-bonding ability of anodically oxidized titanium in rabbits. Biomaterials. 2003;24:4959–66.
17. Hazan R, Brener R, Oron U. Bone growth to metal implants is regulated by their surface chemical properties. Biomaterials. 1993;14:570–4.
18. Degidi M, Nardi D, Piattelli A. 10-year follow-up of immediately loaded implants with TiUnite porous anodized surface. Clin Implant Dent Relat Res. 2012;14:828–38.
19. Fujishima A, Rao TN, Tryk DA. Titanium dioxide photocatalysis. J Photochem Photobiol C Photochem Rev. 2000;1:1–21.
20. Fujishima A, Zhang X, Tryk DA. TiO_2 photocatalysis and related surface phenomena. Surf Sci Rep. 2008;63:515–82.
21. Han Y, Chen D, Sun J, Zhang Y, Xu K. UV-enhanced bioactivity and cell response of micro-arc oxidized titania coatings. Acta Biomater. 2008;4:1518–29.
22. Aita H, Hori N, Takeuchi M, Suzuki T, Yamada M, Anpo M, Ogawa T. The effect of ultraviolet functionalization of titanium on integration with bone. Biomaterials. 2009;30:1015–25.
23. Sunada K, Watanabe T, Hashimoto K. Studies on photokilling of bacteria on TiO_2 thin film. J Photochem Photobiol A Chem. 2003;156:227–33.
24. Zhang H, Banfield JF. Understanding polymorphic phase transformation behavior during growth of nanocrystalline aggregates: insights from TiO_2. J Phys Chem B. 2000;104:3481–7.
25. Cui X, Kim H-M, Kawashita M, Wang L, Xiong T, Kokubo T, Nakamura T. Preparation of bioactive titania films on titanium metal via anodic oxidation. Dent Mater. 2009;25:80–6.

26. Tanaka K, Capule MFV, Hisanaga T. Effect of crystallinity of TiO_2 on its photocatalytic action. Chem Phys Lett. 1991;187:73–6.
27. Kawahara T, Ozawa T, Iwasaki M, Tada H, Ito S. Photocatalytic activity of rutile–anatase coupled TiO_2 particles prepared by a dissolution–reprecipitation method. J Colloid Interface Sci. 2003;267:377–81.
28. Ozawa T, Iwasaki M, Tada H, Akita T, Tanaka K, Ito S. Low-temperature synthesis of anatase–brookite composite nanocrystals: the junction effect on photocatalytic activity. J Colloid Interface Sci. 2005;281:510–3.
29. Hirose F, Ito M, Kurita K. Low-temperature chemical vapor deposition of anatase TiO_2 with titanium tetraisopropooxide and H_2O_2 vapor. Jpn J Appl Phys. 2008;47:5619–22.
30. Chaiyakun S, Pokaipisit A, Limsuwan P, Ngotawornchai B. Growth and characterization of nanostructured anatase phase TiO_2 thin films prepared by DC reactive unbalanced magnetron sputtering. Appl Phys A. 2009;95:579–87.
31. Diamanti MV, Pedeferri MP. Effect of anodic oxidation parameters on the titanium oxides formation. Corr Sci. 2007;49:939–48.
32. Ma C, Nagai A, Yamazaki Y, Toyama T, Tsutsumi Y, Hanawa T, Wang W, Yamashita K. Electrically polarized micro-arc oxidized TiO_2 coatings with enhanced surface hydrophilicity. Acta Biomater. 2012;8:860–5.
33. Arconada N, Durán A, Suárez S, Portela R, Coronado JM, Sánchez B, Castro Y. Synthesis and photocatalytic properties of dense and porous TiO_2-anatase thin films prepared by sol–gel. Appl Catal B Environ. 2009;86:1–7.
34. Kofstad P, Anderson PB, Krudtaa OJ. Oxidation of titanium in the temperature range 800–1200°C. J Less Common Met. 1961;3:89–97.
35. Jamesh M, Kumar S, Narayanan TSNS. Effect of thermal oxidation on corrosion resistance of commercially pure titanium in acid medium. J Mater Eng Perform. 2012;21:900–6.
36. Güleryüz H, Çimenogle H. Effect of thermal oxidation on corrosion and corrosion–wear behaviour of a Ti–6Al–4 V alloy. Biomaterials. 2004;25:3325–33.
37. Dong H, Li XY. Oxygen boost diffusion for the deep-case hardening of titanium alloys. Mater Sci Eng A. 2000;280:303–10.
38. Browne M, Gregson PJ. Surface modification of titanium alloy implants. Biomaterials. 1994;15:894–8.
39. Borgioli F, Galvanetto E, Fossati A, Pradelli G. Glow-discharge and furnace treatments of Ti-6Al-4V. Surf Coat Technol. 2004;184:255–62.
40. Lee K-S, Park I-S. Anatase-phase titanium oxide by low temperature oxidation of metallic Ti thin film. Scr Mater. 2003;48:659–63.
41. Shimada S, Kozeki M. Oxidation of TiC at low temperatures. J Mater Sci. 1992;27:1869–75.
42. Shabalin IL, Roach DL, Shabalin LI. Oxidation of titanium carbide–graphite hetero-modulus ceramics with low carbon content II. Physico-chemical interpretation of the ridge effect. J Eur Ceram Soc. 2008;28:3177–88.
43. Nishikiori H, Takei M, Oki K, Takano S, Tanaka N, Fujii T. Photocatalytic activity of titania layer prepared by oxidizing titanium compounds on titanium plate surface. Appl Catal B Environ. 2012;127:227–33.
44. Kao C-H, Yeh S-W, Huang H-L, Gan D, Shen P. Study of the TiO to anatase transformation by thermal oxidation of Ti film in air. J Phys Chem C. 2011;115:5648–56.
45. Spurr RA, Myers H. Quantitative analysis of anatase-rutile mixtures with an X-ray diffractometer. Anal Chem. 1957;29:760–2.
46. Hanaor DAH, Sorrell CC. Review of the anatase to rutile phase transformation. J Mater Sci. 2011;46:855–74.
47. Kaleji BK, Sarraf-Mamoory R, Fujishima A. Influence of Nb dopant on the structural and optical properties of nanocrystalline TiO_2 thin films. Mater Chem Phys. 2012;132:210–5.
48. Bickley RI, Gonzalez-Carreno T, Lees JS, Palmisano L, Tilley RJD. A structural investigation of titanium dioxide photocatalysts. J Solid State Chem. 1991;92:178–90.

49. Su R, Bechstein R, Sø L, Vang RT, Sillassen M, Esbjörnsson B, Palmqvist A, Besenbacher F. How the anatase-to-rutile ratio influences the photoreactivity of TiO_2. J Phys Chem C. 2011;115:24287–92.
50. Li J, Zhao Y. Biocompatibility and antibacterial performance of titanium by surface treatment. J Coat Technol Res. 2012;9:223–8.
51. Joo H-C, Lim Y-J, Kim M-J, Kwon H-B, Han J-H. Characterization on titanium surfaces and its effect on photocatalytic bactericidal activity. Appl Surf Sci. 2010;257:741–6.
52. Baran N, Starosvetsky D, Starosvetsky J, Epshtein M, Armon R, Ein-Eli Y. Enhanced photo-efficiency of immobilized TiO_2 catalyst via intense anodic bias. Electrochem Commun. 2007;9:1684–8.